



Discovery of novel *Trypanosoma cruzi* glyceraldehyde-3-phosphate dehydrogenase inhibitors

Renato F. Freitas^a, Igor M. Prokopczyk^a, Aderson Zottis^c, Glaucius Oliva^c, Adriano D. Andricopulo^c, Maria Teresa S. Trevisan^b, Wagner Vilegas^d, Maria Goretti V. Silva^{a,b,*}, Carlos A. Montanari^{a,*}

^a Grupo de Estudos em Química Medicinal de Produtos Naturais, NEQUIMED-PN, Instituto de Química de São Carlos, Universidade de São Paulo, 13560-970 São Carlos, SP, Brazil

^b Departamento de Química Analítica e Físico-Química, Departamento de Química Orgânica e Inorgânica, Universidade Federal do Ceará, 60021-970 Fortaleza, CE, Brazil

^c Laboratório de Química Medicinal e Computacional, Centro de Biotecnologia Molecular Estrutural, Instituto de Física de São Carlos, Universidade de São Paulo, 13560-970 São Carlos, SP, Brazil

^d Departamento de Química Orgânica, Universidade Estadual Paulista, 14800-900 Araraquara, SP, Brazil

ARTICLE INFO

Article history:

Received 15 December 2008

Revised 28 January 2009

Accepted 30 January 2009

Available online 13 February 2009

Keywords:

Chagas' disease

Trypanosoma cruzi

GAPDH inhibitors

LBVS

SBVS

ABSTRACT

Based on its essential role in the life cycle of *Trypanosoma cruzi*, the glycolytic enzyme glyceraldehyde 3-phosphate dehydrogenase (GAPDH) has been considered a promising target for the development of novel chemotherapeutic agents for the treatment of Chagas' disease. In the course of our research program to discover novel inhibitors of this trypanosomatid enzyme, we have explored a combination of structure and ligand-based virtual screening techniques as a complementary approach to a biochemical screening of natural products using a standard biochemical assay. Seven natural products, including anacardic acids, flavonoid derivatives, and one glucosylxanthone were identified as novel inhibitors of *T. cruzi* GAPDH. Promiscuous inhibition induced by nonspecific aggregation has been discarded as specific inhibition was not reversed or affected in all cases in the presence of Triton X-100, demonstrating the ability of the assay to find authentic inhibitors of the enzyme. The structural diversity of this series of promising natural products is of special interest in drug design, and should therefore be useful in future medicinal chemistry efforts aimed at the development of new GAPDH inhibitors having increased potency.

© 2009 Elsevier Ltd. All rights reserved.

1. Introduction

For decades, natural products have been considered as a rich source of drugs for a variety of human diseases and disorders.¹ Advances in separation, purification, and high-throughput screening methods have generated increased interest in drug discovery from natural sources. Within the new challenges of the post-genomic era, this field of research is experiencing renewed interest considering the large chemical diversity of natural products and their remarkable range of biological activity.¹

Natural products have played a major role in the chemotherapy of parasitic diseases.² In modern drug research, the interest in natural products remains high as a significant source of new leads and drug candidates for a wide variety of neglected diseases, many of which have received little attention from the pharmaceutical industry. Although screening of natural and synthetic compounds has been extensively used to identify new inhibitors of a number of enzymes, special attention should be paid to the problem of aggregate-based nonspecific inhibition.³ Promiscuous inhibition

is common among natural products at micromolar concentrations, and it is advantageous to remove them from further considerations at the earliest opportunity.

Chagas' disease is a major health problem in several countries of Latin America, and in the southern United States.⁴ The protozoan parasite *Trypanosoma cruzi* is the etiological agent of this devastating disease, which affects millions of people each year. It is thought that at least 25 million people are at risk of infection.⁴ The only two available drugs (nifurtimox and benznidazole) are limited and suffer from several drawbacks such as poor efficacy, toxicity, resistance, and multiple side effects. Therefore, there is an urgent need for the discovery of new, more effective, and safer drugs for human use.⁵

Knowledge of the biochemistry of *T. cruzi* has allowed the identification of new potential targets for chemotherapy intervention. One of such important drug targets receiving considerable attention is the enzyme glyceraldehyde-3-phosphate dehydrogenase (GAPDH; EC 1.2.1.12), a key protein in the glycolytic pathway of trypanosomatids.⁶

Despite their high utility as sources of novel chemical structures, there are only a few natural products reported as inhibitors of *T. cruzi* GAPDH. Thus, the search for new small-molecule inhibitors obtained from natural sources is not only the main goal of the

* Corresponding authors. Tel.: +55 16 33739986; fax: +55 16 33739985 (C.A.M.).
E-mail addresses: mgsilva@ufc.br (M. G. V. Silva), montana@iqsc.usp.br (C.A. Montanari).

present study, but also an important focus of medicinal chemistry research.

2. Results and discussion

2.1. Virtual screening

The compounds assayed in this work were selected from an *in-house* database, which comprehends a set of 220 natural compounds, without any reported activity against *T. cruzi* GAPDH. All compounds were firstly submitted to a pattern recognition analysis. Our strategy consisted of the projection of the *in-house* database over a library model that was constructed from a set of 120 *T. cruzi* GAPDH inhibitors.⁷ This database allowed the identification of crucial structural features for potency, selectivity, and pharmacokinetic properties for *T. cruzi* GAPDH ligands, such as coumarins, flavonoids, and nucleosides.⁷ VOLSURF⁸ was used to construct the library model, employing the DRY, H₂O, and O GRID probes.

It can be seen in Figure 1 that there are roughly three clusters in the PCA score plot, comprising the three chemical classes present in the library of 120 *T. cruzi* GAPDH inhibitors. The vast majority of flavonoids are positioned in the top-left corner of the plot. The coumarins are more concentrated in the center of the graph. The nucleoside/nucleoside-like compounds are located in the right region of the plot.

The chemical structures of compounds 1–9 shown in Figure 2 disclose the activity spectrum for the *T. cruzi* GAPDH inhibitors going from the least to the most potent ones to be distributed toward positive PC1 score values, as depicted in Figure 1. Compounds 7–9 were added in the analysis as the most potent *T. cruzi* GAPDH inhibitors. Their structures and IC₅₀ values can also be found in Figure 2. The IC₅₀ values are in the moderate to low micromolar range, being the nucleoside-like the most potent inhibitors within this series.

We projected our *in-house* collection of natural product compounds over the known GAPDH inhibitors⁷, named here as GAPDH library. As can be seen in Figure 3, the natural products (represented by circles) are distributed according to the chemical–biological space in a similar fashion to the GAPDH library. Although our *in-house* compounds are structurally diverse from the previously reported ones, the virtual chemical probes are equally useful to select promising compounds for biochemical evaluation against *T. cruzi* GAPDH.

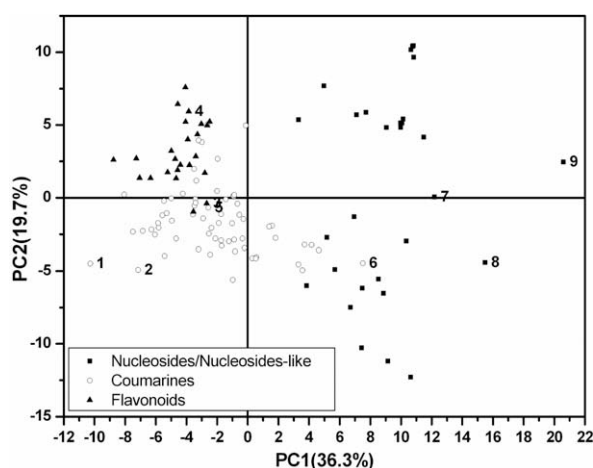


Figure 1. PCA score plot of 120 *T. cruzi* GAPDH ligands. Compounds 1–9 are highlighted to characterize the rank order (least to most potent) of the *T. cruzi* GAPDH inhibitors at high positive PC1 values.

Since the superposition of our *in-house* database is marked by the chemical space that coincides with that of the original GAPDH dataset, we have then selected a diverse subset of 35 natural products to be experimentally assayed against the *T. cruzi* GAPDH enzyme (Fig. 4). These compounds were chosen because they are widespread clustered within the whole range of the PC1 score plot as shown in Figure 4 where activity would be elicited for *T. cruzi* GAPDH inhibition.

2.2. In vitro screening

The preliminary biochemical screening of the 35 natural products (pure substances) against *T. cruzi* GAPDH revealed 7 promising compounds, which were selected for further kinetic evaluation through the determination of IC₅₀ values (compounds 10–16, Fig. 4). The chemical structures and corresponding values of IC₅₀ are depicted in Table 1. The other 28 compounds showed modest or no inhibition at the concentration of 200 μ M (results not shown).

Quercetin and ursolic acid (structure not shown) are among the natural product compounds previously tested against the trypomastigote form of *T. cruzi*, with IC₅₀ values of 771 μ M and 4 μ M, respectively.^{9,10} The obtained IC₅₀ value of quercetin for inhibition of *T. cruzi* GAPDH is 142 μ M.

The trypanocidal activity of the triterpene ursolic acid on trypomastigote form of *T. cruzi* does not correlate with its low *T. cruzi* GAPDH inhibition (about 25% inhibition, for which the IC₅₀ value was not determined). Although both guajaverin and mangiferin have similar potencies to that of quercetin against *T. cruzi* GAPDH, their effects against the trypomastigote form of the parasite remain to be investigated.

Interestingly, the flavonoid tiliroside (11) and the (8*E*,11*E*,14*E*)-anacardic acid (10) have potency in the low micromolar range, with IC₅₀ values of 46 μ M and 38 μ M, respectively. This is a motivating result, since their potencies are lower than the K_M for D-glyceraldehyde-3-phosphate (G3P) and thio-nicotinamide adenine dinucleotide (thio-NAD⁺), which are 270 \pm 15 μ M and 140 \pm 15 μ M, respectively. In addition, tiliroside was active against the amastigote form of *Leishmania amazonensis* and *T. cruzi*, with a percentage of inhibition of 67.8% and 45.0%, respectively (inhibitor concentration of 841 μ M).¹¹

Tiliroside (11) showed promising in vitro effects against Ehrlich tumor cells (IC₅₀ = 69.5 \pm 14.9 μ M). However, this flavonoid is inactive against some human cell lines.¹² Based on that, the finding that tiliroside has a good inhibitory activity against GAPDH is of remarkable interest in the search for novel inhibitors with clinical utility. The potency of 11 is comparable to that of the most potent inhibitors of *T. cruzi* GAPDH, showing its potential as lead for further development.

The discovery of the coumarin chalepin¹³ as a *T. cruzi* GAPDH inhibitor (IC₅₀ = 64 μ M) prompted drug design strategies toward natural product research. Chalepin was the first natural product inhibitor to be crystallized with the *T. cruzi* GAPDH enzyme, allowing the identification of its mode of binding (MOB). The crystal structure of *T. cruzi* GAPDH bound to chalepin shows that the catalytic amino acid Cys166 and others interact with chalepin molecule in the G3P binding site. These interactions preclude the G3P to be transformed to its product—1,3-bisphosphoglycerate (1,3-BPG). Tiliroside (11) and the (8*E*,11*E*,14*E*)-anacardic acid (10) are good examples of natural products that exhibit higher inhibitory potency than chalepin on *T. cruzi* GAPDH.

The C₁₅ anacardic acids have a salicylic acid system and a long side chain at the 6-position of the phenyl ring. There are double bonds that are found at C₈ in the monoene, C₈ and C₁₁ in the diene and C₈, C₁₁, and C₁₄ in the triene side chains. One of the three-anacardic acids acts as a potent inhibitor of *T. cruzi* GAPDH (compound

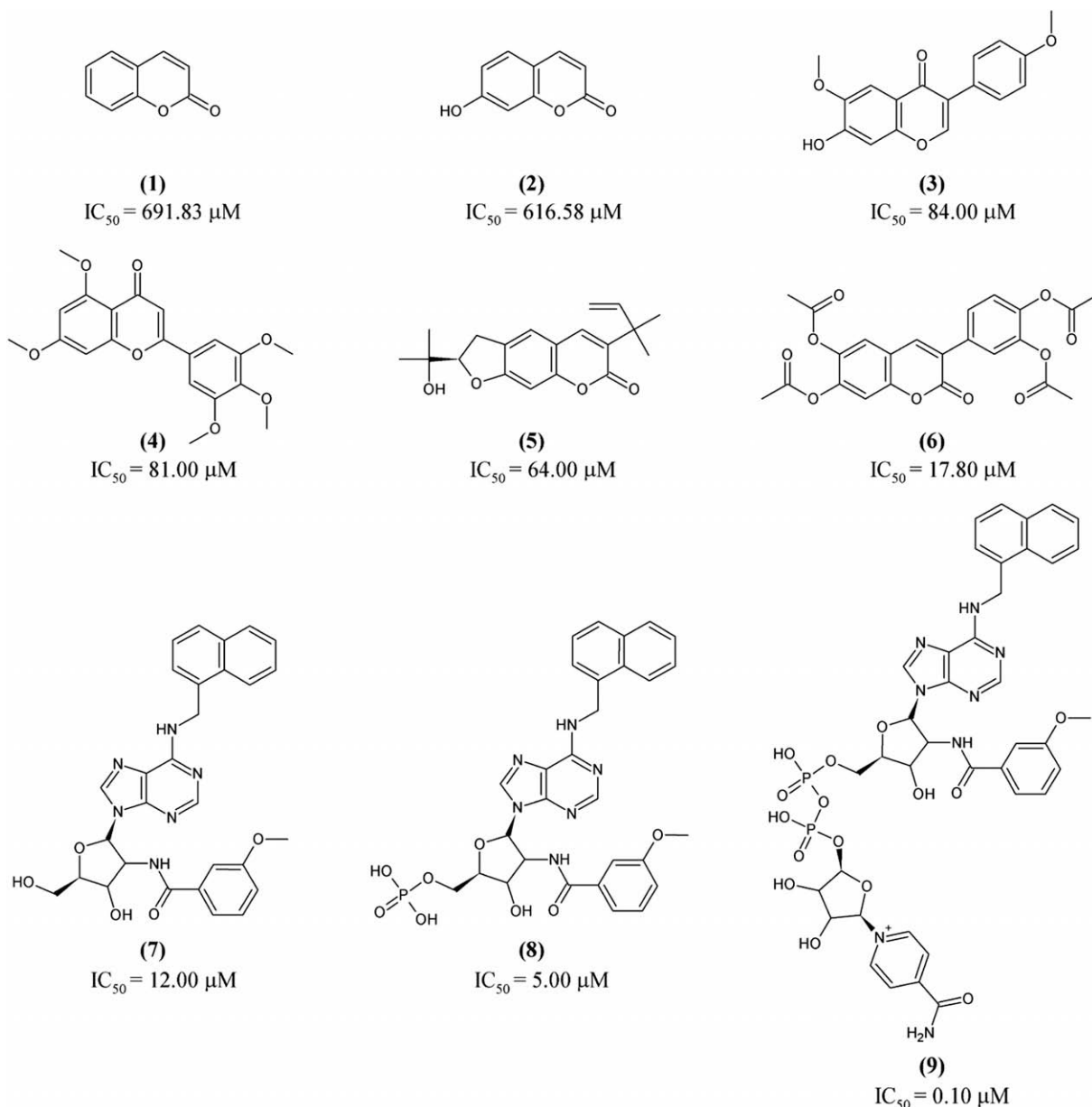


Figure 2. Chemical structures and IC_{50} values of some *T. cruzi* GAPDH inhibitors.

10). Primary studies on the structure–activity relationships (SAR) of the anacardic acids suggest the importance of the double bonds for the inhibitory potency. The most potent anacardic acid (**10**) of the series has three double bonds. These results indicate the potential of this class as promising inhibitors of *T. cruzi* GAPDH. To the best of our knowledge, there is only one previous description of anacardic acid analogs acting as *T. cruzi* GAPDH inhibitors.¹⁴ On the other hand, extracts derived from *Anacardium occidentale*, which contain a mixture of these anacardic acids, showed interesting in vitro activity against *T. cruzi*.¹⁵ Therefore, the compound **10** should be an attractive candidate to be evaluated in vitro and in vivo against different forms of the parasite.

2.3. Nonspecific inhibition

At micromolecular concentrations, some molecules form colloidal aggregates that will non-specifically inhibit enzymes. Such molecules have been termed promiscuous. A possible promiscuous

inhibitory mechanism of compounds **10–16** was checked out by following the effect, if any, of adding Triton X-100 to assay mixtures.¹⁶ This non-ionic surfactant prevents the aggregation of compounds. We found that the degree of inhibition was in all cases unaffected by the presence of Triton X-100, with or without a period of preincubation (data not shown). This proves that inhibition is due to the specific binding of individual molecules to the target enzyme.

2.4. Docking/molecular dynamics study

GAPDH catalyses the oxidation and phosphorylation of G3P to 1,3-BPG in the presence of NAD^+ and inorganic phosphate. Analysis of SAR of tiliroside, guajaverin, and quercetin in the active site of the *T. cruzi* GAPDH revealed consistent docking poses required for a good scoring function. An interesting result is that the docking energy improves in the same order as the IC_{50} values: tiliroside ($-10.50 \text{ kcal mol}^{-1}$, $IC_{50} = 46 \mu M$) > guajaverin

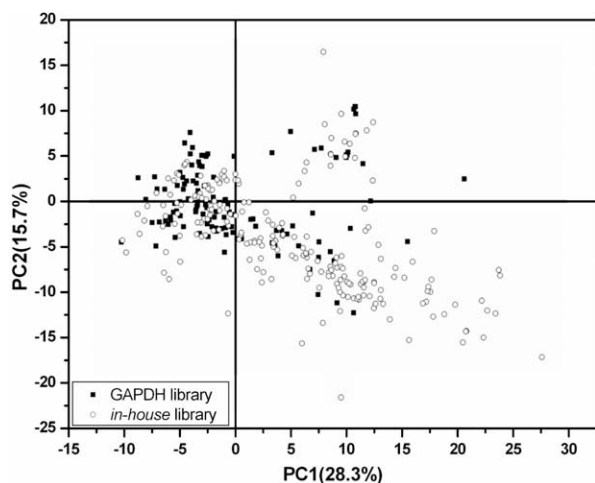


Figure 3. Projection of 220 natural products as potential *T. cruzi* GAPDH inhibitors over the GAPDH library.

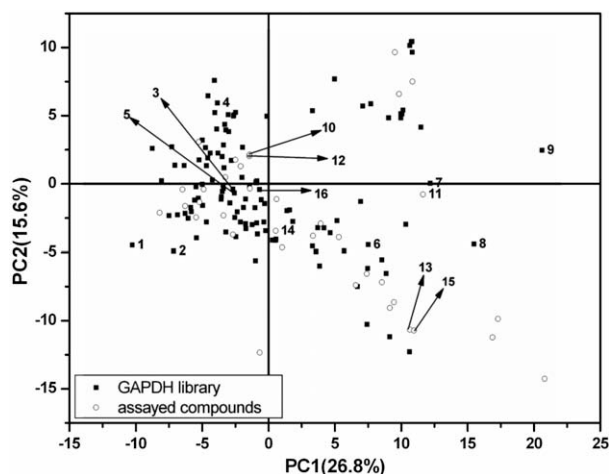


Figure 4. PCA score plot of the projection of 35 natural products as potential *T. cruzi* GAPDH inhibitors over the GAPDH library. The active compounds (10–16) identified in this work are highlighted.

($-8.52 \text{ kcal mol}^{-1}$, $\text{IC}_{50} = 141 \text{ }\mu\text{M}$) > quercetin ($-7.43 \text{ kcal mol}^{-1}$, $\text{IC}_{50} = 143 \text{ }\mu\text{M}$).

The best-ranked pose of each molecule occupies the same region near the catalytic residue (Cys166) in the active site of *T. cruzi* GAPDH (Fig. 5a). In addition, these molecules present parts of their structures within a protein cavity formed by the amino acids: Arg12, Ser195, Tyr196, Thr197, Ala198, Val203, Pro253, Asn335, and Glu336 (Fig. 5b).

Tiliroside is stabilized by four hydrogen bonds with the amino acids Cys166, Ser134, and Ser110. Guajaverin is stabilized by five hydrogen bonds with the amino acids Ser165, Thr226, Arg249, Ser134, and Glu336. Quercetin is stabilized by two hydrogen bonds with the amino acids Ala198 and Pro253. The position of tiliroside and guajaverin would be able to avoid the approach of G3P to Cys166. The side chain of tiliroside extends toward NAD⁺ binding site. A close inspection of Figure 6 reveals that the side chain of tiliroside superposes well with the cofactor NAD⁺. This could also prevent NAD⁺ from making the necessary contacts with the amino acids in its binding site, so avoiding the advancement of the catalysis.

In order to better explore the flexibility of the optimized docking configurations, the best pose of tiliroside was submitted to molecular dynamics experiments using the procedure outlined in

the experimental section. The main interactions of the tiliroside-GAPDH complex observed after the MD simulations are shown in Figure 7. A careful analysis indicates that the configurations obtained for the complex are stable. The active site residues display a conserved orientation, and the key hydrogen bonds between the tiliroside and the enzyme active site are all retained, but the amino acids to which tiliroside makes these interactions are different.

After the MD simulation, three hydrogen bonds were observed between the flavonoid and the amino acids residues Thr167, Thr111, and Glu336. Additionally, as observed in the best docking pose, the side chain of tiliroside extends toward the NAD⁺ binding site. During the MD simulations of the tiliroside-GAPDH complex, the core structure of the flavonoid remains approximately invariable, where the RMSD between the docked structure and the one after MD simulation is 1.65 Å. The main difference was observed in the side chain of tiliroside, which is far away from its initial position (approximately 5.10 Å, as calculated for the oxygen atom bound to the phenyl ring at the tail of tiliroside's side chain).

3. Conclusion

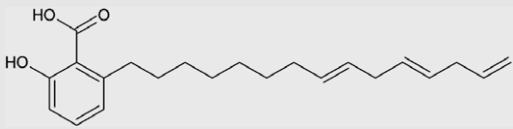
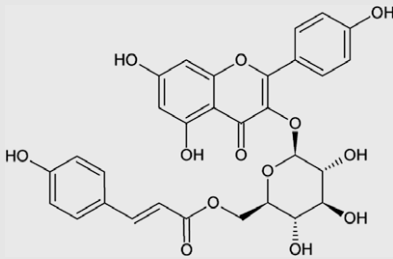
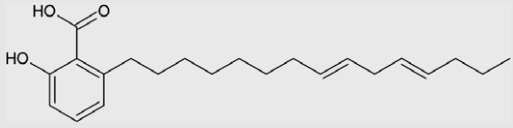
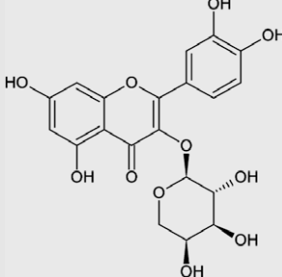
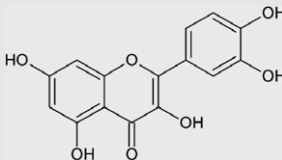
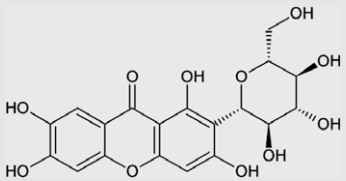
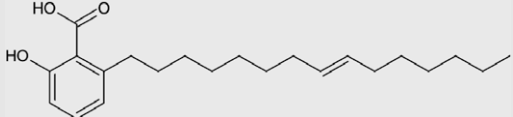
Overall, our combined computational and experimental strategies allowed the identification of a series of *T. cruzi* GAPDH inhibitors as potential trypanocidal agents. Most of the inhibitors identified in the present study represent a new chemical diversity for the target enzyme, and are promising candidates for further optimization and SAR studies. Importantly, the identification of new *T. cruzi* GAPDH inhibitors fulfils a great expectation in the searching for novel drug candidates for the treatment of a long lasting disease called the Chagas' disease.

4. Experimental

4.1. Molecular interaction fields (MIF)

The 3D structures of the database compounds were constructed using CONCORD.¹⁷ Three-dimensional MIF were calculated for the generated 3D conformations using the GRID force field,¹⁸ employing three virtual chemical probes: O (carbonyl), DRY (hydrophobic), and H₂O (water). The carbonyl probe was used for the investigation of specific hydrogen bonding interactions, whereas the hydrophobic DRY probe was used for the study of hydrophobic binding interactions, and, finally, for the identification of hydrophilic regions and corresponding interactions with water molecules, the H₂O probe was employed. The properties of the probes are selected from a table of probe groups. The carbonyl probe is a small and distinct chemical entity represented by carbonyl oxygen. The two hydrogen bonds to it occur near the lone-pair orbitals, which have a charge of -0.25 at an angle of 120° . The hydrophobic probe finds places at which atoms on the surface of a target molecule will make favorable interactions with hydrophobic atoms on another molecule. This hydrophobic probe may be regarded as a modified water probe. Like water, it is able to donate and accept hydrogen bonds, and is electrically neutral. The interaction energy values, however, are calculated in the range of -0.2 to $-1.6 \text{ kcal mol}^{-1}$. The water probe is treated as an extended oxygen atom, and is allowed to donate two hydrogen bonds and to accept two. It will have sp^3 tetrahedral geometry, or sp^2 flat trigonal geometry, or something in between as appropriate. The interaction energy values are computed at eight energy levels ranging from -0.2 to $-6.0 \text{ kcal mol}^{-1}$. VOLSURF is a computational procedure to produce 2D molecular descriptors from 3D interaction energy grid maps. It can be used either for disclosing pharmacokinetic properties of small molecules or for the prediction of protein/small-mol-

Table 1
Chemical structures and IC₅₀ values for a series of natural products as inhibitors of *T. cruzi* GAPDH

Compound	Structure	IC ₅₀ (μM)
(8 <i>E</i> ,11 <i>E</i> ,14 <i>E</i>)-Anacardic acid (10)		38 ± 3
Tiliroside (11)		46 ± 7
(8 <i>E</i> ,11 <i>E</i>)-Anacardic acid (12)		69 ± 9
Guajaverin (13)		140 ± 17
Quercetin (14)		142 ± 13
Mangiferin (15)		149 ± 18
(8 <i>E</i>)-Anacardic acid (16)		161 ± 19

ecule affinity.^{19,20} From the calculated 3D MIF, 2D descriptors are generated by compression of the information content found in the maps. The MIF are calculated around the target molecules and the resulting 2D descriptors are evaluated by multivariate analysis. In this study, the Volsurf 3.0 program was used to calculate the built-in GRID MIF and to analyze the 2D descriptors.

4.2. Docking

The crystal structure of *T. cruzi* GAPDH used in the docking studies was obtained from the Protein Data Bank (1QXS).²¹ The

ligand and crystallographic water molecules were completely removed. For the docking procedures, Gasteiger charges²² were calculated using the AutoDock Tools program (ADT). The receptor model was also prepared with the ADT program through the addition of polar hydrogens, and loading Kollman United Atoms charges.²³ With the use of AutoGrid (part of the AutoDock 3.0.5²⁴ package), affinity grids centered on and encompassing the active site were calculated for the respective ligand atom types with 0.375 Å spacing in a box (70 Å × 60 Å × 60 Å). The torsion and rotatable bonds in the ligands were defined by AutoTors, an auxiliary tool of AutoDock, which also united the nonpolar hydrogens

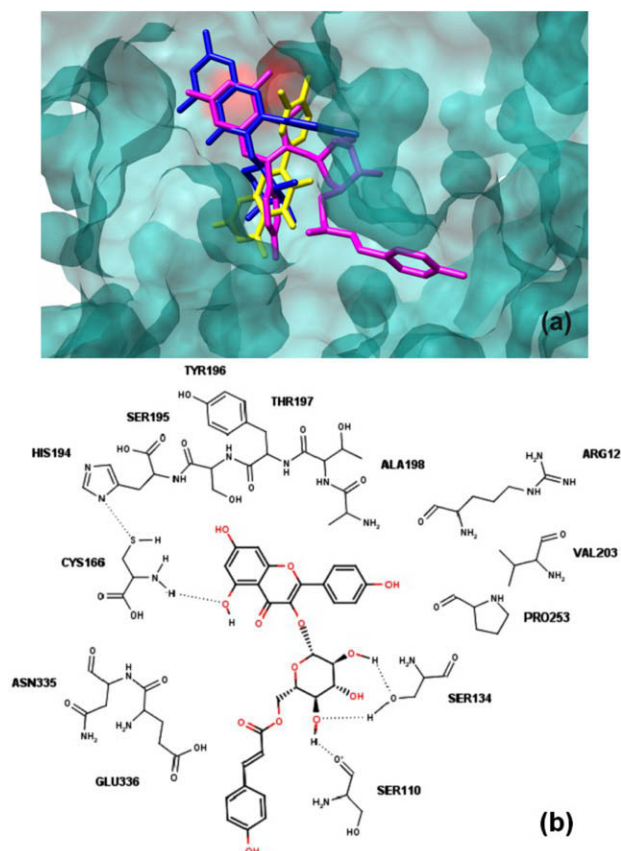


Figure 5. (a) Binding site surface representation of the *T. cruzi* GAPDH, showing the three flavonoids: tiliroside (magenta), guajaverin (blue), and quercetin (yellow). The surface of the amino acid residue Cys166 is shown in red; (b) schematic drawing of the specific interactions between tiliroside and the GAPDH binding site.

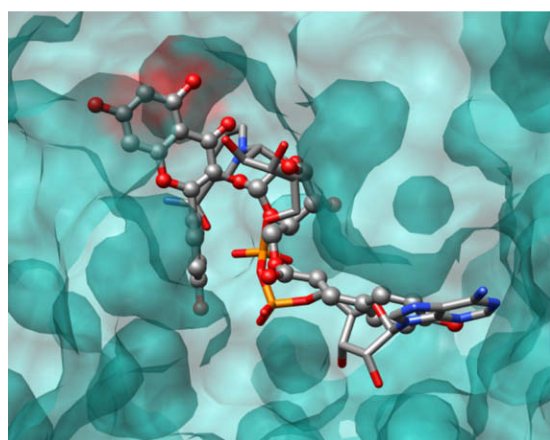


Figure 6. Binding site surface representation of the *T. cruzi* GAPDH, showing the superposition of tiliroside (ball and sticks) and NAD⁺ (sticks) in the crystal structure (PDB ID: 1QXS). The surface of the amino acid residue Cys166 is shown in red.

and partial atomic charges to the bonded carbon atoms. A flexible docking was carried out with AutoDock to evaluate ligand binding energies over the conformational search space using the Lamarckian genetic algorithm. Default docking parameters were used with the following exceptions: ga_pop_size, 500; ga_num_evals, 2500000; ga_num_generations, 270000; and ga_run, 30. The docking conformations of each ligand were clustered based on root-mean-square deviation (RMSD), and ranked based on free energies

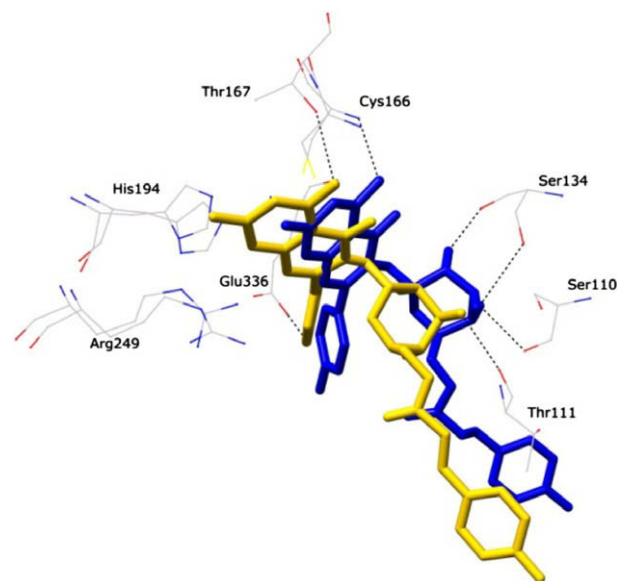


Figure 7. Binding site of *T. cruzi* GAPDH, showing the hydrogen bonds (black dashed line) between the ligand and the amino acids residues of the active site. The docked pose of tiliroside is shown in blue. In gold is its pose obtained after MD simulations.

of binding. The top-ranked conformations were subject to visual inspection.

4.3. Molecular dynamics

The starting conformation for molecular dynamics studies was selected based on the best-ranked conformation of each ligand in the binding site of *T. cruzi* GAPDH, which was obtained using the program AutoDock3.0.5. Each individual complex was minimized using the AMBER force field in the presence of GB/SA continuum water model, before performing the molecular dynamics simulations. The complex was minimized for 3000 steps of Steepest Descent plus 1000 steps of Polak-Ribiere conjugate gradient using the MACROMODEL 9.1 program.²⁵ Hydrogen atoms were constrained to the ideal geometry using the SHAKE algorithm. Nonbonded energy terms were included up to 15 Å for van der Waals interactions and 20 Å for charge–charge electrostatics. All atomic charges were derived from the AMBER force field. For the simulations of the protein–ligand complexes, the residues further away (20 Å) from the Cys166 were constrained by harmonic constraints, while the other residues were allowed to move freely in the sphere. An initial random velocity to all atoms corresponding to 300 K was applied. At this point, the rigid part of the system was kept frozen and the thermalization of the mobile part was started by running four molecular dynamics simulations: initial temperature of 500 K; cooling down of 100 K at 10 ps with 1.5 fs time step up to 200 K. The molecular dynamics was carried out at constant temperature (298 K) for 2 ns and 1.5 fs time step. The conformations (40) from molecular dynamics runs were fully minimized for 500 steps of conjugate gradient. All molecular dynamics were carried out by using the MACROMODEL 9.1 program.

4.4. Expression and purification of glycosomal *T. cruzi* GAPDH

Expression and purification of glycosomal *T. cruzi* GAPDH protein expression and purification were carried out as described previously.^{26,27} Briefly, culture of *Escherichia coli* with recombinant *T. cruzi* GAPDH was incubated and the expression of this enzyme was then induced under specific conditions. After this procedure, the

cells were lysed and centrifuged. The resulted supernatant was fractionated and the mixture was centrifuged. The supernatant was fractionated and the mixture again centrifuged. The supernatant was purified by hydrophobic chromatography and the eluted fractions subsequently purified by cation-exchange chromatography. The concentration of GAPDH was achieved by further dialysis against TEA buffer using an Amicon concentrator to achieve the final concentration of 9 mg mL⁻¹. Purity of the protein was checked and monitored by SDS–PAGE.

4.5. Kinetic measurements

Kinetic measurements were carried out spectrophotometrically with the aid of a Cary 100 UV–Vis spectrophotometer equipped with a Peltier-thermostatted multicell changer and a temperature controller, using a standard assay. All experiments were carried out in triplicate at 25 °C. The reaction mixture contained 100 mM triethanolamine, HCl buffer 590 (pH 7.5), 1 mM EDTA, 1 mM 2-mercaptoethanol, 30 mM NaHAsO₄·7H₂O, 250 μM thio-NAD⁺, 300 μM D-glyceraldehyde-3-phosphate, and appropriate amounts of *T. cruzi* GAPDH enzyme (usually 40 nM) and ligands (natural products). The final reaction volume was 1 mL, kept under stirring. All kinetic measurements were performed under initial velocity conditions. The biochemical reduction of thio-NAD⁺ to thio-NADH ($\epsilon = 11.9 \times 10^3 \text{ M}^{-1} \text{ cm}^{-1}$) was monitored at 405 nm for 8 min, which is equivalent to about 8% reduction of thio-NAD⁺. The percentage of inhibition was calculated according to the following equation:

$$\% \text{ Inhibition} = 100 \times (1 - v_i/v_0)$$

where v_i and v_0 are the initial velocities (enzyme activities) determined in the presence and in the absence of inhibitor, respectively. Values of IC₅₀ were independently determined by making rate measurements for at least six inhibitor concentrations. The values represent means of at least three individual experiments. The kinetic parameters were estimated from the collected data employing the Sigma-Plot enzyme kinetics module.

4.6. Nonspecific inhibition assays

Nonspecific inhibition was evaluated in the presence of Triton X-100. A stock solution 1% (v/v) of the detergent was freshly prepared in triethanolamine, HCl buffer (pH 7) with EDTA and 2-mercaptoethanol to achieve the equivalent concentration in the cuvette as the same for assay reaction. The volume of this solution (5 μL) was then added to perform 0.01% of Triton in the reaction mixture; a concentration that was first evaluated and showed no interference with enzymatic activity. During the assays, this solution was added to the mixture through two procedures. First, the addition was made right after putting in the compound. Second,

the compound was added, followed by Triton X-100 and then the enzyme.

Acknowledgments

We are indebted to CNPq (Conselho Nacional de Desenvolvimento Científico e Tecnológico) and FAPESP (Fundação de Amparo à Pesquisa do Estado de São Paulo), for financial support and scholarships.

References and notes

- Beghyn, T.; Poulain, R. D.; Willand, N.; Folleas, B.; Deprez, B. *Chem. Biol. Drug Des.* **2008**, 72, 3.
- Kayser, O.; Kiderlen, A. F.; Croft, S. L. *Parasitol. Res.* **2003**, 90, 55.
- Coan, K. E. D.; Shoichet, B. K. *J. Am. Chem. Soc.* **2008**, 130, 9606.
- Liñares, G. E. G.; Ravaschino, E. L.; Rodriguez, J. B. *Curr. Med. Chem.* **2006**, 13, 335.
- Maya, J. D.; Cassels, B. K.; Vásques, P. I.; Ferreira, J.; Faundez, M.; Galantini, N.; Ferreira, A.; Morello, A. *Comp. Biochem. Physiol. Part A* **2007**, 146, 601.
- Ladame, S.; Castilho, M. S.; Silva, C. H. T. P.; Denier, C.; Hannaert, V.; Périé, J.; Oliva, G.; Willson, M. *Eur. J. Biochem.* **2003**, 270, 4574.
- Leitão, A.; Andricopulo, A. D.; Oliva, G.; Pupo, M. T.; Marchi, A. A.; Vieira, P. C.; Silva, M. F. G. F.; Ferreira, V. F.; Souza, M. C. B. V.; Sá, M. M.; Moraes, V. R. S.; Montanari, C. A. *Bioorg. Med. Chem. Lett.* **2004**, 14, 2199.
- Cruciani, G.; Pastor, M.; Guba, W. J. *Med. Chem.* **2000**, 43, 2204.
- Contini, S. H. T.; Salvador, M. J.; Balanco, J. M. F.; Albuquerque, S.; de Oliveira, D. C. R. *Phytother. Res.* **2004**, 18, 250.
- Taketa, A. T. C.; Gnoatto, S. C. B.; Gosmann, G.; Pires, V. S.; Schenke, E. P.; Guillaume, D. J. *Nat. Prod.* **2004**, 67, 1697.
- Schinor, E. C.; Salvador, M. J.; Pral, E. M. F.; Alfieri, S. C.; Albuquerque, S.; Dias, D. A. *Braz. J. Pharm. Sci.* **2007**, 43, 295.
- Esteves-Souza, A.; Silva, T. M. S.; Alves, C. C. F.; Carvalho, M. G.; Braz-Filho, R.; Echevarria, A. J. *Braz. Chem. Soc.* **2002**, 13, 838.
- Pavão, F.; Castilho, M. S.; Pupo, M. T.; Dias, R. L.; Correa, A. G.; Fernandes, J. B.; da Silva, M. F.; Mafezoli, J.; Vieira, P. C.; Oliva, G. *FEBS Lett.* **2002**, 520, 13.
- Pereira, J. M.; Severino, R. P.; Vieira, P. C.; Fernandes, J. B.; da Silva, M. F. G. F.; Zottis, A.; Andricopulo, A. D.; Oliva, G.; Correa, A. G. *Bioorg. Med. Chem.* **2008**, 16, 8889.
- Luize, P. S.; Tiuman, T. S.; Morello, L. G.; Maza, P. K.; Ueda-Nakamura, T.; Dias Filho, B. P.; Cortez, D. A. G.; Mello, J. C. P.; Nakamura, C. V. *Braz. J. Pharma. Sci.* **2005**, 41, 85.
- Feng, B. Y.; Shoichet, B. K. *Nat. Protoc.* **2006**, 1, 550.
- CONCORD 5.11; Tripos Inc., 1699 South Hanley Road, St. Louis, MO 63144.
- Wade, R. C.; Clark, K. J.; Goodford, P. J. *J. Med. Chem.* **1993**, 36, 140.
- Zamora, I.; Oprea, T.; Cruciani, G.; Pastor, M.; Ungell, A. L. *J. Med. Chem.* **2003**, 46, 25.
- Menezes, I. R. A.; Lopes, J. C. D.; Montanari, C. A.; Oliva, G.; Pavão, F.; Castilho, M. S.; Vieira, P. C.; Pupo, M. T. *J. Comput.-Aided Mol. Des.* **2003**, 17, 277.
- Ladame, S.; Castilho, M. S.; Silva, C. H.; Denier, C.; Hannaert, V.; Perie, J.; Oliva, G.; Willson, M. *Eur. J. Biochem.* **2003**, 270, 4574.
- Gasteiger, J.; Marsili, M. *Org. Magn. Reson.* **1981**, 15, 353.
- Weiner, S. J.; Kollman, P. A.; Nguyen, D. T.; Case, D. A. *J. Comput. Chem.* **1986**, 7, 230.
- Goodsell, D. S.; Morris, G. M.; Olson, A. J. *J. Mol. Recognit.* **1996**, 9, 1.
- MACROMODEL 9.1; Schrodinger, LLC: New York, 2007.
- Vellieux, F. M.; Hajdu, J.; Verlinde, C. L. M. J.; Groendijk, H.; Read, R. J.; Greenhough, T. J.; Campbell, J. W.; Kalk, K. H.; Littlechild, J. A.; Watson, H. C.; Hol, W. G. J. *Proc. Natl. Acad. Sci. U.S.A.* **2003**, 90, 2355.
- Hannaert, V.; Opperdoes, F. R.; Michels, P. A. M. *Protein Exp. Purif.* **1995**, 6, 244.